Effective viscous flow and transport in a tube with corrugated surface

Gerardo Severino [*]
Division of Water Resources Management and Biosystems Engineering, University of Naples – Federico II, Piazza Carlo di Borbone, 1 - I80055, Portici (NA), Italy

(Received 22 January 2025; accepted 10 June 2025; published 2 July 2025)

We consider viscous flow and solute transport in a tube with a corrugated surface, whose topology cannot be accurately described due to either a scarcity of data or measurement errors (or, more frequently, both). This uncertainty can be addressed by modeling the geometry of the roughness as a stationary random field. Consequently, flow and transport equations become stochastic. To solve these equations, the irregular boundary of the flow domain is mapped onto a smooth one (no roughness), with the impact of the original geometry encapsulated in the components of the contravariant tensor associated with the mapping. A perturbation expansion is then employed to compute the statistics of the velocity field, which is used to derive the effective viscosity and quantify the diffusion mechanism of an advected passive solute. It is observed that the effective viscosity depends on the degree of disorder in the roughness geometry and, therefore, cannot be regarded solely as a property of the fluid. Instead, the concentration is shown to satisfy a diffusion-type equation with time-dependent effective parameters. In particular, the effective diffusion coefficient converges to a constant (asymptotic) value after a transitional period, which depends on the correlation scale of the random signal describing the surface topology. The analytical nature of the solutions allows for the treatment of surfaces with, among other characteristics, short correlation lengths—an issue that cannot be effectively addressed using Monte Carlo simulations.

DOI: 10.1103/mjj4-4trl

I. INTRODUCTION

In recent years, the influence of corrugated (irregular) boundaries on Stokes flow, and consequently on solute transport, has been systematically neglected. This is because the irregular geometry of the hosting domain was assumed to have a minor impact due to its relatively large size. However, advancements in new technologies have made it possible to study flows influenced by grooved surfaces. This has permitted tackling a wide range of problems relevant in physics, such as chaotic mixing [1], small-scale hydrodynamics [2], and cancer propagation [3]. The significance of this topic also lies in its universal nature, as surface shape affects phenomena as diverse as these [2]. Indeed, any natural (or even manufactured) domain is inherently irregular, and this irregularity influences flow and transport processes within it. This class of problems has been approached via two main avenues: one involving simplified mathematical models and another that introduces appropriate boundary conditions to account for the impact of the domain's geometry (see, e.g., [4–6]). In both cases, however, the irregular (and not deterministically known) topology of the boundaries is replaced by a smooth one. In contrast, this study examines viscous flow in a tube with a surface topology that cannot be described exactly due to limited information and/or measurement errors. This situation calls for a probabilistic description of the irregular surfaces to enable a

[*]Contact author: gerardo.severino@unina.it

computationally feasible solution to the problem [7–9]. Specifically, we propose a methodology for averaging Stokes flow and solute transport, following an approach similar to that of Tartakovsky and Xiu [10]. However, while these authors employed a numerical, approximate procedure based on polynomial chaos expansion, we adopt an analytical (perturbation) approach. This method allows us to address surfaces with small correlation lengths—an issue that cannot be resolved by computer simulations (for a general overview, see, e.g., [11]). Central to the framework developed in this study is the use of a mapping that transforms a differential equation (or a system of equations) defined on a random domain into a stochastic differential equation with regular boundaries, thereby enabling the use of standard solution techniques (similarly to [12]).

A key problem in the theory of stochastic processes is determining the constitutive laws that govern the mean values of flow and transport variables. Specifically, the challenge lies in deriving the effective properties. Similar problems arise in various branches of fluid physics, such as viscous and turbulent flows and/or the advection and mixing of scalars in porous formations. In these cases, the stochastic nature of the fields stems from the velocity, that is treated as a given random field (a comprehensive exposition can be found in [13,14]). Instead, in the present study, the random nature of the variables is due to the irregular geometry of the boundary conditions. The key step is the selection of a proper mapping which translates the grooved domain into a regular one, while the stochastic nature of the walls is shifted into the coefficients of the new governing equation(s).

We demonstrate that the parameter, termed effective viscosity, which replaces the homogeneous velocity profile with the mean one, depends on the heterogeneity of the wall's roughness. Consequently, it cannot be considered solely a property of the fluid. In the case of transport, we aim to quantify the spreading mechanism induced by the irregular topology of the tube walls. For a smooth tube (ideal topology), the concentration would follow the classical advection-diffusion equation with constant coefficients [15]. In contrast, the irregular topology generates additional spreading that is directly tied to the degree of heterogeneity of the tube walls, rather than to the diffusion coefficient. This behavior is analogous to the enhanced dispersion observed during transport in heterogeneous porous formations (similarly to the enhanced dispersion observed in transport through heterogeneous porous formations, [13]).

The structure of the paper is as follows: We model the geometry of the tube walls as a stationary Gaussian random field and map the initial (irregular) domain into a smooth one. We then employ a perturbation expansion to solve the resulting stochastic system of partial differential equations. This solution yields the expression for the effective viscosity. Finally, we address the transport of a passive scalar and, similarly to flow, compute effective parameters for the advection-diffusion equation. We conclude with final remarks.

II. THE FLOW PROBLEM AND PERTURBATION SOLUTION

We consider the steady Stokes flow of an incompressible fluid of viscosity μ taking place in a tube of variable radius r (Fig. 1). The velocity field $\boldsymbol{v} \equiv (\mathrm{v}^1, \mathrm{v}^2, \mathrm{v}^3)^\top$ and pressure p satisfy the system formed by the momentum and continuity equations, i.e.,

$$\begin{cases} \mu\, \nabla^2 \mathrm{v}^i - \dfrac{\partial p}{\partial x_i} = -\delta_{i,2}\,\gamma, & \text{(1a)} \\ \nabla \cdot \boldsymbol{v} = 0, & \text{(1b)} \end{cases}$$

being γ the specific (per unit volume) gravitational force. Moreover, in Eqs. (1a) and (1b), we assume that $i = 1, 2, 3$ with the convention that $x_3 \equiv z$ in $\boldsymbol{x} \equiv (x_1, x_2, x_3)$. If the tube were smooth, the radius r would be equal to the constant value R, and the system (1a) and (1b) would give rise to the well-known Hagen-Poiseuille's velocity profile:

$$\mathrm{v}^3(r) = -\frac{\gamma R^2}{4\mu}\frac{\partial h}{\partial z}\left[1 - \left(\frac{r}{R}\right)^2\right], \quad h = \frac{p}{\gamma}, \quad r = \sqrt{x_1^2 + x_2^2}. \tag{2}$$

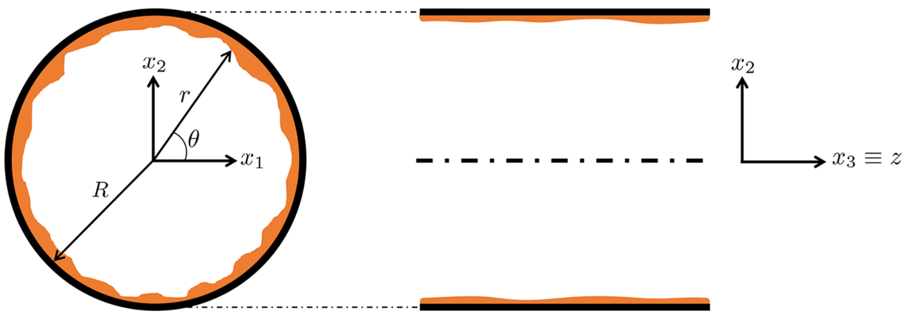

FIG. 1. Cross section (left) and longitudinal view (right) of a tube (radius R) with corrugated (orange face) surface.

Now, we cast the problem (1a) and (1b) in a dimensionless form by rescaling the coordinates and variables as follows: $\hat{\boldsymbol{x}} = \boldsymbol{x}/R$, $\hat{r} = r/R$, $\hat{\boldsymbol{v}} = \mu \boldsymbol{v}/(\gamma R^2)$ and $h = h/R$. As a consequence, (1a) and (1b) are replaced with

$$\begin{cases} \hat{\nabla}^2 \hat{\mathrm{v}}^i - \dfrac{\partial \hat{h}}{\partial \hat{x}_i} = -\delta_{i,2}, & \text{(3a)} \\ \hat{\nabla} \cdot \hat{\boldsymbol{v}} = 0. & \text{(3b)} \end{cases}$$

Hereafter, we drop the "hat symbol" to simplify the notation.

The corrugated geometry of the wall introduces small-scale fluctuations (orange face in Fig. 1) along the surface that *de facto* reduce the effective tube's radius. This makes the problem more difficult as compared with its smooth counterpart, since now the geometry of the domain $\Gamma = \{(r, \theta, z) : 0 \leqslant r \leqslant 1 - \varepsilon, 0 \leqslant \theta \leqslant 2\pi, z \in \mathbb{R}\}$ is affected by the parameter $0 \leqslant \varepsilon < 1$. The fluctuations of the signal ε can be accounted for by regarding the latter as the realization ω of a random field, whose statistical parameters can be inferred by measurements. Moreover, by following a frequently adopted assumption [see, e.g., [16], and references therein], ε is sought as a weakly (spatially) variable signal such that one can postulate $\mathbb{P}\{0 \leqslant \varepsilon \ll 1\} = 1$. A possible solution strategy for this problem is to map Γ onto a new domain A of regular boundaries by means of the change of variable: $\boldsymbol{\xi} = r\,\frac{\cos\theta}{1-\varepsilon}\,\boldsymbol{e}_1 + r\,\frac{\sin\theta}{1-\varepsilon}\,\boldsymbol{e}_2 + z\,\boldsymbol{e}_3$. Then, by accounting for the rules of transformation [see, e.g., [17]] of the derivatives from one framework to another, system (3a) and (3b) writes as

$$\begin{cases} |\bar{g}|^{-1/2} \dfrac{\partial}{\partial \xi^j}\left(G^{jk} \dfrac{\partial \mathrm{v}^i}{\partial \xi^k} \right) - \dfrac{\partial h}{\partial \xi^i} = -\delta_{i,2}, \quad G^{jk} = g^{jk} |\bar{g}|^{1/2}, & \text{(4a)} \\ \dfrac{\partial}{\partial \xi^k}(\mathrm{v}^k |\bar{g}|^{1/2}) = 0, \quad \bar{g} = \det(g_{jk}), \quad \boldsymbol{\xi} \equiv (\xi^1, \xi^2, \xi^3) \in A, & \text{(4b)} \end{cases}$$

(summation convention over $j, k = 1, 2, 3$ is adopted). The fundamental feature of the new system (4a) and (4b) is that now the flow domain $A \equiv [0, 1] \times [0, 2\pi] \times \mathbb{R}$ is smooth, with the original impact of the corrugated tube's surface incorporated in the contravariant components g^{jk} (that are coefficients).

To identify the covariant components g_{jk} which lead to the contravariant tensor, we start from the metric $\mathrm{d}s^2 \equiv \mathrm{d}\boldsymbol{\xi} \cdot \mathrm{d}\boldsymbol{\xi}$, being the total differential given by $\mathrm{d}\boldsymbol{\xi} = \mathrm{d}\Lambda_i \boldsymbol{e}_i$

$$\mathrm{d}\Lambda_1 = \mathrm{d}r\,\frac{\cos\theta}{1-\varepsilon} + \mathrm{d}\theta\, r \frac{\partial}{\partial\theta}\left(\frac{\cos\theta}{1-\varepsilon}\right) + \mathrm{d}z\, r \frac{\partial}{\partial z}\left(\frac{\cos\theta}{1-\varepsilon}\right), \tag{5}$$

$$\mathrm{d}\Lambda_2 = \mathrm{d}r\,\frac{\sin\theta}{1-\varepsilon} + \mathrm{d}\theta\, r \frac{\partial}{\partial\theta}\left(\frac{\sin\theta}{1-\varepsilon}\right) + \mathrm{d}z\, r \frac{\partial}{\partial z}\left(\frac{\sin\theta}{1-\varepsilon}\right), \tag{6}$$

$$\mathrm{d}\Lambda_3 = \mathrm{d}z. \tag{7}$$

As a consequence, the components $g_{\eta\nu}$ $(\eta, \nu \equiv r, \theta, z)$ of the covariant tensor result from $\mathrm{d}s^2 = g_{\eta\nu}\mathrm{d}x^\eta \mathrm{d}x^\nu$ as

$$g_{rr} = \frac{1}{(1-\varepsilon)^2}, \quad g_{\theta\theta} = \frac{r^2}{(1-\varepsilon)^4}\left[(1-\varepsilon)^2 + \left(\frac{\partial \varepsilon}{\partial \theta}\right)^2\right], \quad g_{zz} = 1 + \frac{r^2}{(1-\varepsilon)^4}\left(\frac{\partial \varepsilon}{\partial z}\right)^2, \tag{8}$$

$$g_{r\theta} \equiv g_{\theta r} = \frac{2r\partial\varepsilon/\partial\theta}{(1-\varepsilon)^3}, \quad g_{rz} \equiv g_{zr} = \frac{2r\partial\varepsilon/\partial z}{(1-\varepsilon)^3}, \quad g_{\theta z} \equiv g_{z\theta} = \frac{2r^2}{(1-\varepsilon)^4}\frac{\partial\varepsilon}{\partial\theta}\frac{\partial\varepsilon}{\partial z}. \tag{9}$$

In particular, for $\varepsilon \to 0$ the only nonvanishing terms in Eqs. (8) and (9) are $g_{rr} = g_{zz} = 1$, $g_{\theta\theta} = r^2$, in agreement with the classical (smooth) formulation of the problem at stake.

Since $\mathbb{P}\{0 \leqslant \varepsilon \ll 1\} = 1$, the quantity $1 - \varepsilon > 0$ is mapped onto the second-order stationary random field $w \equiv w(\boldsymbol{\xi}; \omega)$ as follows: $w = -\ln(1-\varepsilon)$. As a matter of fact, the system (4a) and (4b) becomes stochastic, and we aim at deriving the equations satisfied by the mean values of the flow variables. Prior to the computation of the contravariant tensor (g^{jk}), it is convenient to rewrite (8) and (9) by recalling that $1 - \varepsilon = \exp(-w)$, the final result being

$$g_{rr} = \exp 2w, \quad g_{\theta\theta} = (r\exp w)^2\left[1 + \left(\frac{\partial w}{\partial\theta}\right)^2\right], \quad g_{zz} = 1 + r^2\left(\frac{\partial}{\partial z}\exp w\right)^2, \tag{10}$$

$$g_{r\theta} = -r\frac{\partial}{\partial\theta}\exp 2w, \quad g_{rz} = -r\frac{\partial}{\partial z}\exp 2w, \quad g_{\theta z} = 2r^2\left(\frac{\partial}{\partial\theta}\exp w\right)\left(\frac{\partial}{\partial z}\exp w\right). \tag{11}$$

Hence, the contravariant components are $g^{jk} = \mathscr{C}(g_{jk})/|\bar{g}|$, where $\mathscr{C}(\cdot)$ is the operator of tensorial conjugation. To simplify the mathematical effort required to compute explicitly the tensor (G^{ij}), we neglect the nonlinear terms in the derivatives appearing into (10) and (11), an approximation which is reasonable in view of the perturbation expansion that will be adopted later on. Hence, it yields

$$(g^{jk}) = \bar{g}^{\,-1/2}\begin{pmatrix} r & -2\frac{\partial w}{\partial\theta} & 0 \\ -2\frac{\partial w}{\partial\theta} & r^{-1} & 0 \\ 0 & 0 & r\exp 2w \end{pmatrix}, \tag{12}$$

being $|\bar{g}|^{1/2} = r\exp 2w$. The utility of the representation (12) stems from the fact that the tensor in the brackets on the right-hand side corresponds to the tensor (G^{ij}). Hereafter, we regard w as a random, weak signal, an assumption that allows expanding the flow variables in an asymptotic series of w, i.e.,

$$\boldsymbol{v} \simeq \sum_m \boldsymbol{v}_{(m)}, \quad h \simeq \sum_m h_{(m)}, \quad m = 0, 1, 2, \ldots, \tag{13}$$

being $\boldsymbol{v}_{(m)}$ and $h_{(m)}$ the m – order corrections to the velocity and head field, respectively. Insertion of (13) into (4a) and (4b), and collecting the same order terms leads to the following sequence of systems:

$$\begin{cases} \left(|\bar{g}|_{(0)}^{-1/2}\dfrac{\partial}{\partial\xi^j}G_{(0)}^{jk}\dfrac{\partial}{\partial\xi^k}\right)\mathrm{v}_{(m)}^i - \dfrac{\partial h_{(m)}}{\partial\xi^i} = -L_{(m)}^i, & \text{(14a)} \\ \dfrac{\partial}{\partial\xi^k}\left(\mathrm{v}_{(m)}^k|\bar{g}|_{(0)}^{1/2}\right) = -Q_{(m)}, & \text{(14b)} \end{cases}$$

$(m = 0, 1, 2)$. It is easy to show that the operators on the left-hand side of (14a) and (14b) coincide with the Laplacian and the divergence in the $\boldsymbol{\xi}$ (i.e., cylindrical) framework, respectively. As for the quantities on the right-hand side, at the leading order, it yields $L_{(0)}^i \equiv \delta_{i,2}$ and $Q_{(0)} = 0$, whereas at the first and second order, one has

$$L_{(1)}^i \equiv \frac{\partial \mathrm{v}_{(0)}^i}{\partial\xi^j}\sum_{n=0}^{1}\frac{\partial G_{(1-n)}^{jk}}{\partial\xi^k}|\bar{g}|_{(n)}^{-1/2}, \quad Q_{(1)} \equiv \mathrm{v}_{(0)}^3\frac{\partial|\bar{g}|_{(1)}^{1/2}}{\partial\xi^3}, \tag{15}$$

and

$$L^i_{(2)} \equiv \frac{\partial \mathrm{v}^i_{(1)}}{\partial \xi^j} \sum_{n=0}^{1} \frac{\partial G^{jk}_{(1-n)}}{\partial \xi^k} |\bar{g}|^{-1/2}_{(n)} + \frac{\partial \mathrm{v}^i_{(0)}}{\partial \xi^j} \sum_{n=0}^{2} \frac{\partial G^{jk}_{(2-n)}}{\partial \xi^k} |\bar{g}|^{-1/2}_{(n)},$$

$$Q_{(2)} \equiv \mathrm{v}^3_{(0)} \frac{\partial |\bar{g}|^{1/2}_{(2)}}{\partial \xi^3} + \frac{\partial}{\partial \xi^k}\left(\mathrm{v}^k_{(1)} |\bar{g}|^{1/2}_{(1)}\right), \tag{16}$$

respectively. It is worth noting that the above expansions can be regarded as a Reynolds's decomposition $T = \langle T \rangle + T'$ in which the leading-order approximation is the mean value, i.e., $\langle T \rangle \equiv T_{(0)}$, whereas the fluctuation is the first-order one, i.e., $T' \equiv T_{(1)}$. To compute the corrections $\boldsymbol{v}_{(n)} \equiv (\mathrm{v}^r_{(n)}, \mathrm{v}^\theta_{(n)}, \mathrm{v}^z_{(n)})$ (with $n = 1, 2$) to the leading order (18), we assume, similarly to the zero-order approximation, that $v^r_{(n)} = v^\theta_{(n)} \simeq 0$ due to the axial-symmetric structure of the flow (such an approximation is seldom adopted in the theory of lubrication flows, see, e.g., [18]). As a consequence, the system (14a) and (14b) may be written as

$$\begin{cases} \nabla^2_c \, \mathrm{v}^z_{(n)} - \dfrac{\partial h_{(n)}}{\partial z} = -L^z_{(n)}, & (17a) \\ r \, \dfrac{\partial}{\partial z} \, \mathrm{v}^z_{(n)} = -Q_{(n)}, & (17b) \end{cases}$$

($n = 1, 2$), being ∇^2_c the Laplacian in cylindrical coordinates (r, θ, z). In particular, from (17b), one gets (we omit the straightforward algebraic details) $\mathrm{v}^z_{(n)} = (-1)^{2-n}\, 2\, \mathrm{v}^\star \mathrm{v}^z_{(0)} w^n$, with

$$\mathrm{v}^z_{(0)}(r) = -\mathsf{J}(1 - r^2), \quad \mathsf{J} \equiv \frac{\partial h_{(0)}}{\partial z} < 0, \quad \mathrm{v}^\star = \frac{\gamma}{\mu} R^2. \tag{18}$$

Thus, the velocity is a stationary random field in the subdomain $(\theta, z) \in [0, 2\pi] \times \mathbb{R}$, solely. This was expected, since $\mathrm{v}_{(0)}$ depends upon the distance r (a general discussion on this topic can be found in [19]). In order to investigate the uncertainty distribution of the velocity along the cross section, in Fig. 2, we have depicted the variance $\sigma^2_{\mathrm{v}} \equiv (2\mathrm{v}^\star \mathrm{v}^z_{(0)} \sigma_w)^2$ as a function of r. It vanishes at the boundary, due to the no-slip condition, whereas the maximum value $\sigma^2_{\mathrm{v,\,max}} = (2\mathrm{v}^\star \mathrm{v}^z_{(0),\mathrm{max}} \sigma_w)^2$ is attained along the tube's axis. The variance σ^2_{v}, together with the leading order approximation (18), provides a quantitative assessment of the uncertainty associated to the velocity field. Moreover, since $\mathrm{v}^z_{(n)} \sim w^n$, the velocity field results are Gaussian.

III. APPLICATIONS

In what follows, we make use of results achieved so far to study two problems that are relevant in the *Physical Review Fluids*, namely the computation of effective properties of viscous flow and tracer transport [20]. Besides being of definite theoretical interest, effective properties can be used to simulate the upscaled version of the same problem. As a consequence, they lend themselves as a useful benchmark for validating more involved numerical codes.

A. Computation of the effective viscosity

In the theory of effective fluid mechanics [see, e.g., [21]], one aims at identifying the parameter (termed viscosity μ_{eff}) which allows us to replace in (18) the homogeneous (no heterogeneity) flow variables with their ensemble averages, i.e.,

$$\langle \boldsymbol{v} \rangle = \frac{-\gamma R^2}{4\mu_{\mathrm{eff}}}\left[1 - \left(\frac{r}{R}\right)^2\right]\boldsymbol{E}, \quad \boldsymbol{E} \equiv \left\langle \frac{\partial h}{\partial z} \right\rangle \boldsymbol{e}_z, \tag{19}$$

where $\boldsymbol{e}_z \equiv (0, 0, 1)^\top$ denotes the unit vector along the z-axis. Thus, μ_{eff} is the quantity that a naive observer would detect from viscometer measurement(s) if the tube's walls were regarded as smooth.

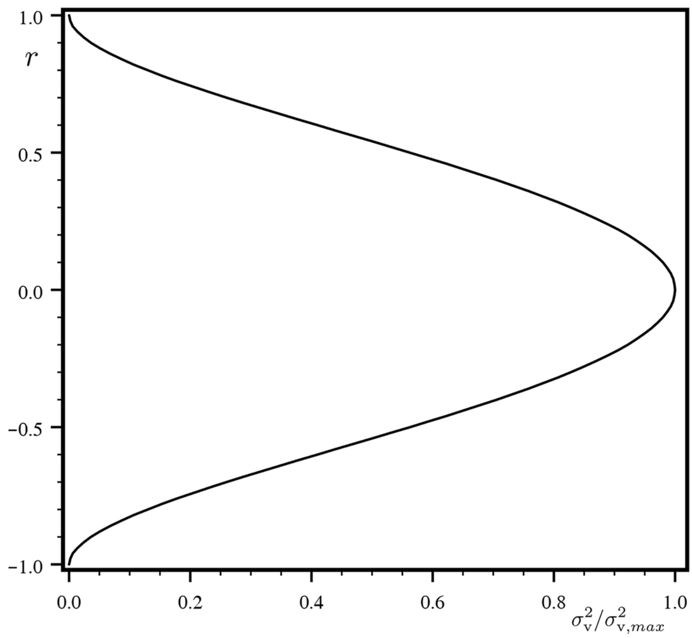

FIG. 2. Dependence upon the normalized radius r of the nondimensional variance $\sigma_{\mathrm{v}}^2/\sigma_{\mathrm{v,\,max}}^2$ along the cross section.

Since

$$\langle \boldsymbol{v} \rangle \equiv \boldsymbol{v}_{(0)} + \langle \boldsymbol{v}_{(2)} \rangle = \left(1 + 2\sigma_w^2\right) \mathrm{v}^\star \mathrm{v}_{(0)}^z \boldsymbol{e}_z, \quad \left\langle \frac{\partial h}{\partial z} \right\rangle = \frac{\partial h_{(0)}}{\partial z} + \left\langle \frac{\partial h_{(2)}}{\partial z} \right\rangle = \mathsf{J}\left(1 + 20\sigma_w^2\right), \tag{20}$$

it is clear that Eq. (19) lends itself as a tool to compute the effective viscosity. In fact, upon "dot multiplication" by $\boldsymbol{e}_z$ on both sides in the first of (19) and accounting for the second of (19), it leads to

$$\langle \boldsymbol{v} \rangle \cdot \boldsymbol{e}_z = \frac{-\gamma R^2}{4\mu_{\mathrm{eff}}} \left[1 - \left(\frac{r}{R}\right)^2\right] \boldsymbol{E} \cdot \boldsymbol{e}_z \Rightarrow \mu_{\mathrm{eff}} = \mu \frac{1 + 20\sigma_w^2}{1 + 2\sigma_w^2}. \tag{21}$$

The effective viscosity, unlike μ, depends also upon the degree of irregularity (i.e., the variance $\sigma_w^2 \equiv \langle w^2 \rangle$ of the random signal w) of the walls' geometry. It results in monotonic increasing with σ_w^2 and it approaches μ for $\sigma_w^2 \to 0$ (Fig. 3), in agreement with the classical result. We can state that the stochastic mapping $\boldsymbol{\xi}_w \mapsto \boldsymbol{\xi}_w(r, \theta, z)$ translates (in the ensemble average sense) the impact of the corrugated walls into an extra (viscous-type) friction.

Although the second of (21) is formally restricted to a topology such that $\sigma_w^2 \ll 1$, it is argued (by the same reasoning of [22]) that it applies to a broader range of the variance σ_w^2 due to the compensation effects of the truncation errors arising from the perturbation expansion. Another relevant property of μ_{eff} is that it is independent of the autocorrelation ρ_w, and concurrently upon the integral scale(s) of heterogeneity of the random signal w. The impact of ρ_w is expected to play in from the third order in σ_w^2 [23], and therefore the influence of the scale(s) of heterogeneity has to be regarded as a higher-order effect [in line with [24]], who reached a similar conclusion by using a different approach]. It is seen (Fig. 4) that the mean velocity (19) is damped more and more with increasing σ_w^2. This effect (similar to that observed in the viscous flow between two parallel rough plates, [16]), resembles the reduction in the velocity profile due to the turbulence [25]. Finally, the volumetric flow rate Q, and concurrently the averaged (along the cross section Σ) velocity $\bar{V} = Q/\Sigma$, are given by $Q = \pi R^4 |\mathsf{J}| \gamma/(8\mu_{\mathrm{eff}})$ and $\bar{V} = R^2 |\mathsf{J}| \gamma/(8\mu_{\mathrm{eff}})$.

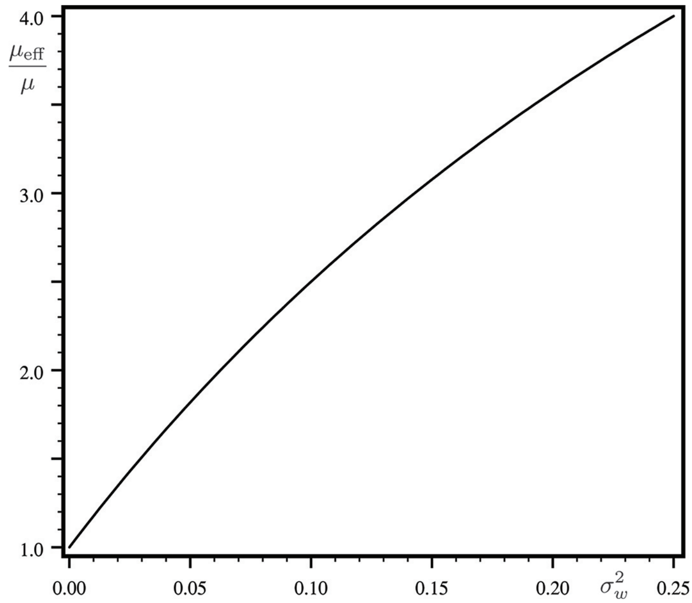

FIG. 3. Dependence of the scaled, effective viscosity μ_{eff}/μ upon the variance σ_w^2.

B. Effective solute transport

Advection-diffusion processes in viscous flows have received significant attention due to their utility in numerous applications [18]. For the flow under consideration, the irregular topology of

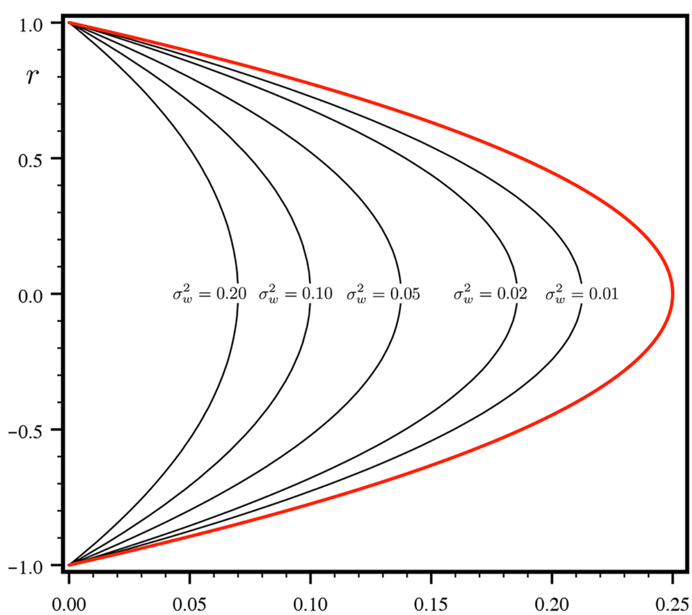

FIG. 4. Nondimensional profile of the magnitude $|\langle \boldsymbol{v} \rangle|/(|\mathsf{J}|\, \mathrm{v}^\star)$ of the mean velocity as a function of r, and several values of the variance σ_w^2. Thick red line pertains to $\sigma_w^2 \equiv 0$ (no roughness).

the walls introduces additional spreading, which would not occur if the tube were ideal. In the advective regime (large Peclet number), where the contribution of Fickian diffusion is assumed to be marginal (an exhaustive discussion on this point can be found in [13], ch. 2.10.2), transport is modeled starting from the leading and first-order approximation of the displacement $X_z \equiv X_z(t)$ of a fluid particle that begins its propagation at $X_z(0) = 0$, i.e.,

$$X_z^{(n)}(t) \equiv \int_0^t \mathrm{d}\tau\, \mathrm{v}_{(n)}^z(\tau), \quad X_z^{(n)} \sim O(w^n), \quad (n = 0, 1, 2). \tag{22}$$

Since at the σ_w^2-order the velocity field is Gaussian, inspection of (22) shows that the same is true for the displacement X_z, whose statistics are therefore completely characterized by the first and second order moments:

$$R_z(t) \equiv X_z^{(0)}(t) = \Sigma^{-1} \int_\Sigma \mathrm{d}\sigma \int_0^t \mathrm{d}\tau\, \mathrm{v}^\star \mathrm{v}_{(0)}^z(\tau) = -\frac{\mathrm{J}}{2}\mathrm{v}^\star t,$$

$$S_z(t) \equiv \left\langle X_z^{(1)\,2}(t)\right\rangle = \Sigma^{-1} \int_\Sigma \mathrm{d}\sigma \int_0^t \int_0^t \mathrm{d}\tau' \mathrm{d}\tau''\, C_\mathrm{v}(\tau', \tau''), \tag{23}$$

respectively. In Eq. (23), the velocity covariance $C_\mathrm{v}(t', t'') \equiv \langle \mathrm{v}_{(1)}^z(r_1, \theta_1, \mathrm{v}^\star t')\mathrm{v}_{(1)}^z(r_2, \theta_2, \mathrm{v}^\star t'')\rangle$ is the longitudinal one (i.e., $r_1 = r_2 = r$ and $\theta_1 = \theta_2 = \theta$). Thus, substitution of the fluctuation $\mathrm{v}_{(1)}^z = -2\,\mathrm{v}^\star\, \mathrm{v}_{(0)}^z w$ gives

$$C_\mathrm{v}(t', t'') = 4[\mathrm{J}\mathrm{v}^\star \sigma_w (1 - r^2)]^2 \langle w(r, \theta, t') w(r, \theta, t'')\rangle = 4[\mathrm{J}\mathrm{v}^\star \sigma_w (1 - r^2)]^2 \rho_w \left(0, 0, \frac{\mathrm{v}^\star}{\ell}|t' - t''|\right), \tag{24}$$

where ℓ is the integral scale of the random signal w. Hence, insertion of the latter into S_z and carrying out the straightforward quadratures leads to

$$S_z(t) = \frac{8}{3}(\mathrm{J}\ell\sigma_w)^2 \int_0^{t/t_c} \mathrm{d}\tau \left(\frac{t}{t_c} - \tau\right)\rho_w(\tau), \tag{25}$$

being the time-scale t_c equal to $\ell/\mathrm{v}^\star$. Note that we have replaced $\rho_w(0, 0, \tau) \mapsto \rho_w(\tau)$ for conciseness of notation. While the first-order moment R_z increases linearly with time, S_z exhibits two distinct regimes:

$$S_z(t) \sim \begin{cases} t^{\star 2} & \text{for } t^\star \ll 1 \ \text{(early time regime)} \\ t^\star & \text{for } t^\star \gg 1 \ \text{(large time regime).} \end{cases} \tag{26}$$

Once R_z and S_z are derived, one can compute the mean concentration $\bar{C}(z, t) = \Sigma^{-1} \int_\Sigma \mathrm{d}\sigma\, C(z, t; \sigma)$. Following an approach similar to that used for the effective viscosity concept, $\bar{C}$ is shown to satisfy the classical advection-diffusion equation:

$$\frac{\partial \bar{C}}{\partial t} + V_\mathrm{eff}(t)\frac{\partial \bar{C}}{\partial z} = D_\mathrm{eff}(t)\frac{\partial^2 \bar{C}}{\partial z^2}, \tag{27}$$

where the effective velocity $V_\mathrm{eff} \equiv V_\mathrm{eff}(t)$ and diffusion coefficient $D_\mathrm{eff} \equiv D_\mathrm{eff}(t)$ are defined as

$$V_\mathrm{eff}(t) = \frac{\mathrm{d}}{\mathrm{d}t} R_z(t), \quad D_\mathrm{eff}(t) = \frac{1}{2}\frac{\mathrm{d}}{\mathrm{d}t} S_z(t). \tag{28}$$

Substituting the expressions (23) and (25) into (28) provides

$$V_\mathrm{eff}(t^\star) = -\frac{\mathrm{J}}{2}\,\mathrm{v}^\star, \quad D_\mathrm{eff}(t^\star) = \frac{4}{3}\,\ell\, \mathrm{v}^\star (\mathrm{J}\sigma_w)^2 \frac{\mathrm{d}}{\mathrm{d}t^\star} \int_0^{t^\star} \mathrm{d}\tau\, (t^\star - \tau)\, \rho_w(\tau). \tag{29}$$

The effective diffusion coefficient is shown to depend on time t, and therefore the so-called dispersivity $\alpha(t) \equiv D_\mathrm{eff}/V_\mathrm{eff}$ can not be regarded as a medium's (i.e., local) property. As it will

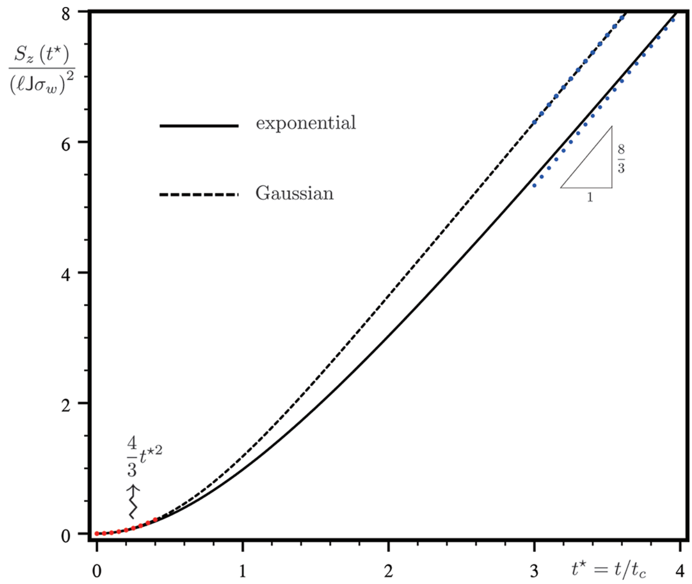

FIG. 5. Dependence of the scaled second–order moment $S_z(t)/(J\ell\sigma_w)^2$ upon the nondimensional time $t^\star = t/t_c$. Dashed and continuous lines refer to Gaussian and exponential ρ_w, respectively. The early (red symbols) and large (blue symbols) approximations of S_z are also quoted.

be shown later, $D_{\text{eff}}(t)$ is an increasing function of t, and it levels on its asymptotic value $D_{\text{eff}}(\infty)$ (Fickian regime). The latter is computed in a general manner by means of Tauber's theorem as follows:

$$D_{\text{eff}}(\infty) \equiv \lim_{t\to\infty} D_{\text{eff}}(t) = \lim_{s\to 0} s\,\hat{D}_{\text{eff}}(s) = \frac{4}{3}\,\ell v^\star (J\sigma_w)^2 \hat{\rho}_w(0) = \frac{4}{3}\,\ell v^\star (J\sigma_w)^2 \int_0^\infty d\alpha\ \rho_w(\alpha)$$
$$= \frac{4}{3}\,\ell v^\star (J\sigma_w)^2, \tag{30}$$

(any ρ_w), where we have used the definition of Laplace transform $\hat{D}_{\text{eff}}(s) = \int_0^\infty dt\, \exp(-st)\, D_{\text{eff}}(t)$ of the effective diffusion coefficient, and employed the convolution theorem. In a different manner, one could state that when the center of gravity R_z has covered a distance equal to $\alpha(\infty) = D_{\text{eff}}(\infty)/V_{\text{eff}} = -(8/3)J\ell\sigma_w^2$, then transport can be simulated by means of an advection-diffusion equation with constant coefficients [26]. In this last case, the difference with the classical (smooth walls) approach stems from the fact that the diffusion coefficient depends upon σ_w^2. Closed form expressions for S_z (25) are easily obtained after selecting the type of the autocorrelation ρ_w (exponential and Gaussian in the present study), the final result being $S_z(t^\star) = (8/3)(J\ell\sigma_w)^2\Phi(t^\star)$, with

$$\Phi(t) = \begin{cases} t + \exp(-t) - 1 & \text{exponential,} \\ t\,\mathrm{erf}\big(\frac{\sqrt{\pi}}{2}\,t\big) - \frac{2}{\pi}\big[1 - \exp\big(-\frac{\pi}{4}\,t^2\big)\big] & \text{Gaussian.} \end{cases} \tag{31}$$

The dependence of $S_z(t^\star)/(J\ell\sigma_w)^2$ upon time $t^\star = t/t_c$ has been depicted in Fig. 5. As the solute propagates, the longitudinal dispersion grows monotonically with time. The early (red symbols) as well as large (blue symbols) time regimes are those predicted by (26): A quadratic dependence in the early regime, whereas for $t^\star \gg 1$, S_z grows linearly (slope $8/3$). By the same token, the ratio

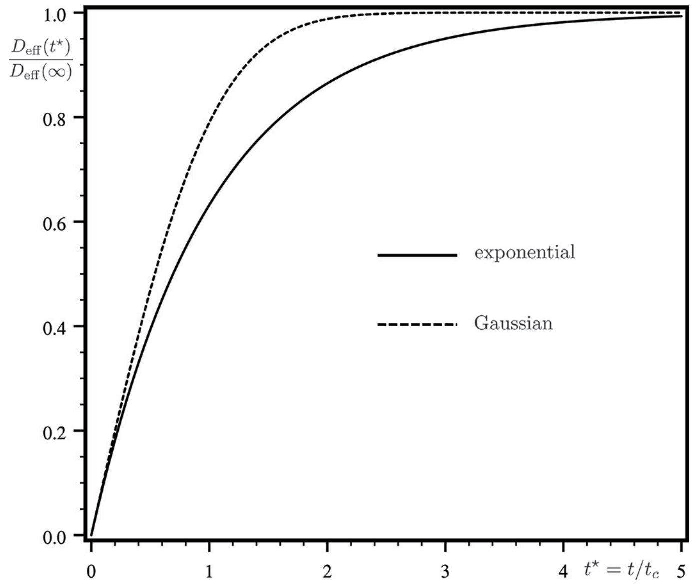

FIG. 6. Nondimensional effective diffusion coefficient $D_{\rm eff}(t)/D_{\rm eff}(\infty)$ as a function of the scaled time $t^\star = t/t_c$. Dashed and continuous lines refer to Gaussian and exponential ρ_w, respectively.

$D_{\rm eff}(t^\star)/D_{\rm eff}(\infty)$ has been calculated by means of (29), i.e.,

$$\frac{D_{\rm eff}(t^\star)}{D_{\rm eff}(\infty)} = \begin{cases} 1 - \exp(-t^\star) & \text{exponential,} \\ \mathrm{erf}\left(\frac{\sqrt{\pi}}{2}\, t^\star\right) & \text{Gaussian,} \end{cases} \tag{32}$$

and it is shown as a function of $t^\star$ (Fig. 6). A relevant feature is the (onset) time for $D_{\rm eff}(t^\star)$ to reach the asymptotic $D_{\rm eff}(\infty)$, from which it is seen that transport can be regarded definitively Fickian when $t \gtrsim 5t_c$.

IV. CONCLUSIONS

We have analyzed Stokes flow and solute transport within a tube characterized by corrugated walls. By modeling the surface topology as a Gaussian, stationary random field, we developed a methodology that enables mapping the actual domain onto a smooth one. In this way, the effects of the irregular geometry, determined by the wall roughness, are transferred from the boundaries to the coefficients in the transformed Stokes equations, thereby allowing the use of standard solution methods. Notably, the analytical nature of our solution, unlike Monte Carlo simulations, allows us to address cases where the characteristic length scale of the random signal is very short. These results provide a framework to address two key problems in the effective theory of fluid mechanics.

(1) *Effective viscosity* ($\mu_{\rm eff}$):

It is the parameter that relates the mean velocity to the mean pressure gradient. It is derived in a simple (closed) form and, consistent with similar findings in the study of flow through randomly heterogeneous porous media, is shown to depend solely on σ_w^2. The influence of the autocorrelation function, ρ_w, is expected to appear only at higher-order approximations.

(2) *Effective velocity* ($V_{\rm eff}$) and *diffusion coefficient* ($D_{\rm eff}$):

These parameters are used in the classical advection-diffusion equation to compute the averaged concentration. Unlike $\mu_{\rm eff}$, $D_{\rm eff}$ depends on travel time for a given autocorrelation function of the random signal, w. After a transitional period, roughly five times the characteristic time scale t_c, the effective diffusion coefficient reaches its asymptotic (constant) value. From this point onward, transport can be described by the advection-diffusion equation with constant coefficients (Fickian regime).

It is noted that results achieved in the present study are limited to the assumption of weak heterogeneity ($\sigma_w^2 \ll 1$). One possible way to relax such a limitation (when accounting for walls with a corrugated surface characterized by a high degree of variability) is by means of the so-called self-consistent approximation [see, e.g., [27]]. This goal might be achieved by a proper conformal mapping and subsequent application of the potential theory. Alternatively, one may adapt the methodology developed by [28] for effective heat flow properties in bounded domains.

ACKNOWLEDGMENTS

This work was supported by the Departmental Fund, Project No. 3778/2022, and by the Italian Ministry of University and Research under Grant No. P2022WC2ZZ (PRIN). The constructive comments from the AE and the Referees have been appreciated, and they have significantly improved the early version of the manuscript.

DATA AVAILABILITY

No data were created or analyzed in this study.

[1] A. D. Stroock, S. K. Dertinger, A. Ajdari, I. Mezic, H. A. Stone, and G. M. Whitesides, Chaotic mixer for microchannels, Science **295**, 647 (2002).

[2] S. Kim and S. J. Karrila, *Microhydrodynamics: Principles and Selected Applications* (Butterworth-Heinemann, Stoneham, 2013).

[3] Y. Dong, A. M. Skelley, K. D. Merdek, K. M. Sprott, C. Jiang, W. E. Pierceall, J. Lin, M. Stocum, W. P. Carney, and D. A. Smirnov, Microfluidics and circulating tumor cells, J. Mol. Diagn. **15**, 149 (2013).

[4] C. Pozrikidis, Unsteady viscous flow over irregular boundaries, J. Fluid Mech. **255**, 11 (1993).

[5] M. Blyth and C. Pozrikidis, Heat conduction across irregular and fractal-like surfaces, Int. J. Heat Mass Transf. **46**, 1329 (2003).

[6] M. Madadi and M. Sahimi, Lattice Boltzmann simulation of fluid flow in fracture networks with rough, self-affine surfaces, Phys. Rev. E **67**, 026309 (2003).

[7] S. W. Park, M. Intaglietta, and D. M. Tartakovsky, Impact of endothelium roughness on blood flow, J. Theor. Biol. **300**, 152 (2012).

[8] S.-W. Park, M. Intaglietta, and D. M. Tartakovsky, Impact of stochastic fluctuations in the cell free layer on nitric oxide bioavailability, Front. Comput. Neurosci. **9**, 131 (2015).

[9] C. Kwon and D. M. Tartakovsky, Modified immersed boundary method for flows over randomly rough surfaces, J. Comput. Phys. **406**, 109195 (2020).

[10] D. M. Tartakovsky and D. Xiu, Stochastic analysis of transport in tubes with rough walls, J. Comput. Phys. **217**, 248 (2006).

[11] D. Xiu and D. M. Tartakovsky, Numerical methods for differential equations in random domains, SIAM J. Sci. Comput. **28**, 1167 (2006).

[12] M. Zayernouri, S.-W. Park, D. M. Tartakovsky, and G. E. Karniadakis, Stochastic smoothed profile method for modeling random roughness in flow problems, Comput. Methods Appl. Mech. Eng. **263**, 99 (2013).

[13] G. Dagan, *Flow and Transport in Porous Formations* (Springer-Verlag GmbH & Co. KG., 1989).

[14] S. B. Pope, *Turbulent Flows* (Cambridge University Press, 2000).

[15] G. I. Taylor, Dispersion of soluble matter in solvent flowing slowly through a tube, Proc. R. Soc. London A **219**, 186 (1953).

[16] G. Severino, Effect of random roughness on Stokes flow, J. Fluid Mech. **1000**, R1 (2024).

[17] G. B. Arfken and H. J. Weber, *Mathematical Methods for Physicists*, 6th ed. (Academic Press, San Diego, 2005).
[18] J. Happel and H. Brenner, *Low Reynolds Number Hydrodynamics: With Special Applications to Particulate Media*, Vol. 1 (Springer Science & Business Media, 2012).
[19] G. Severino and S. Cuomo, Uncertainty quantification of unsteady flows generated by line-sources through heterogeneous geological formations, SIAM/ASA J. Uncertainty Quantif. **8**, 807 (2020).
[20] T. C. Choy, *Effective Medium Theory: Principles and Applications*, Vol. 165 (Oxford University Press, 2015).
[21] B. Noetinger, L. Hume, R. Chatelin, and P. Poncet, Effective viscosity of a random mixture of fluids, Phys. Rev. Fluids **3**, 014103 (2018).
[22] I. Jankovic, A. Fiori, and G. Dagan, Effective conductivity of an isotropic heterogeneous medium of lognormal conductivity distribution, Multiscale Model. Simul. **1**, 40 (2003).
[23] A. De Wit, Correlation structure dependence of the effective permeability of heterogeneous porous media, Phys. Fluids **7**, 2553 (1995).
[24] A. Zarlenga, I. Janković, A. Fiori, and G. Dagan, Effective hydraulic conductivity of three-dimensional heterogeneous formations of lognormal permeability distribution: The impact of connectivity, Water Resour. Res. **54**, 2480 (2018).
[25] C. S. Jog, *Fluid Mechanics*, Vol. 2 (Cambridge University Press, 2015).
[26] R. Aris, On the dispersion of a solute in a fluid flowing through a tube, Proc. R. Soc. London A **235**, 67 (1956).
[27] G. Severino, F. De Paola, and G. Toraldo, Dipole-flow disturbed by a circular inclusion of conductivity different from the background: From deterministic to a self-consistent analytical solution, Phys. Rev. Fluids **7**, 064101 (2022).
[28] A. Rabinovich, G. Dagan, and T. Miloh, Boundary effects on effective conductivity of random heterogeneous media with spherical inclusions, Phys. Rev. E **86**, 046601 (2012).